New insights into time synchronization of MIMO systems without and with interference

Sonja Hiltunen, Pascal Chevalier, Titouan Petitpied

NEW INSIGHTS INTO TIME SYNCHRONIZATION OF MIMO SYSTEMS WITHOUT AND WITH INTERFERENCE

Sonja Hiltunen[1], Pascal Chevalier[2,3] and Titouan Petitpied[3]

(1) Dialogue Technologies, 481 Viger Avenue West, Montréal QC H2Z 1G6, Canada

(2) CNAM, Laboratoire CEDRIC, Hesam University, 292 rue Saint-Martin, 75141 Paris Cédex 3, France

(3) Thales-Communications-Security, HTE/AMS/TCP, 4 Av. Louvresses, 92622 Gennevilliers, Cédex, France

Tel : +1438 921 8705 , sonhya@gmail.com,

Tel : (33) – 1 40 27 24 85, pascal.chevalier@cnam.fr, pascal.chevalier@thalesgroup.com

Tel : (33) – 1 46 13 20 83, titouan.petitpied@thalesgroup.com

February 2019

ABSTRACT

The time synchronization of (*M*x*N*) MIMO systems has been studied this last fifteen years, for both single-carrier (SC) and multi-carriers links. Without any interference, most of the available receivers assume orthogonal sequences. With interference, the current most powerful receiver is a generalized likelihood ratio test (GLRT) receiver, assuming unknown, stationary, circular, temporally white and spatially colored Gaussian noise. However, this receiver is more complex than its non-GLRT counterparts, which, unfortunately, do not perform as well in most cases. In this context, the purpose of this paper is to get new insights into the time synchronization of SC MIMO links, both without and with interference, in order to overcome the limitations of the available receivers. In the absence of interference, the MIMO GLRT receiver is computed and compared to the existing ones in a unified framework, enlightening its better performance. In the presence of interference, as the complexity is an important issue in practice, several ways to decrease the complexity of the available GLRT receiver while keeping its performance are proposed, enlightening the great practical interest of the proposed schemes. Finally, the optimization of the number of transmit antennas is investigated, enlightening the existence of an optimal value of *M* depending on the channel matrix.

Keywords : *Time Synchronization, MIMO, SIMO, GLRT, MMSE, Interference.*

1. INTRODUCTION

Two decades ago, MIMO systems, which use multiple antennas at both transmitter and receiver, were developed to increase the throughput (bit rate) and reliability of communications over fading channels through spatial multiplexing [1] [2] and space-time coding (STC) [3] [4] at transmission, without the need of increasing the receiver bandwidth. This powerful technology has been adopted in several wireless standards such as IEEE 802.11n, IEEE 802.16 [5], LTE [6] or LTE-Advanced [7] in particular. Nevertheless, as wireless spectrum is an expensive resource, increasing network capacity without requiring additional bandwidth is a great challenge for wireless networks. This has motivated the development of multi-user MIMO (MU-MIMO) techniques [8], such as Interference Alignment techniques [9], allowing several MIMO links to share the same time-frequency resource. However, in order to be efficient, all these MIMO links require a preliminary step of time and frequency synchronization which has to be also robust to interference.

Time and frequency synchronization of MIMO systems have been strongly studied these last fifteen years, mainly in the contexts of direct-sequence coded division multiple acces (DS-CDMA) and orthogonal frequency division multiplex (OFDM) links. Both coarse and fine time synchronization jointly with frequency offset estimation and compensation have been analyzed, and many techniques have been proposed either for time-frequency synchronization [10-21] or for time synchronization only [22-32]. Nevertheless, most of these techniques assume both an absence of interference, i.e. a temporally and spatially white noise, and orthogonal synchronization sequences. On the other hand, the scarce papers of the literature dealing with MIMO synchronization in the presence of interference, i.e. for a temporally white but spatially colored noise, correspond to [16] [28] [30] [31]. More precisely, [16] and [28] consider the problem of MIMO synchronization in the presence of multi-user interference (MUI) only. The proposed techniques exploit the known structure of MUI and are not robust to external interference such as hostile jammers, which may be a great limitation for military applications in particular. The unique paper dealing with MIMO synchronization in the presence of interference of any kind, such as hostile jammers, has been published recently and corresponds to [30]. In [30], several receivers are proposed for time synchronization in both flat fading and frequency selective fading channels. However, for complexity reasons, only those developed for flat fading channels seem to be realistic for practical situations. Note that in practice, a receiver which is developed for flat fading channels may also be used for frequency selective channels, considering the secondary propagation multi-paths as interference. Two receivers which are robust to interference of any kind have been proposed in [30] for flat fading channels. They are derived from a minimum mean square error (MMSE) and a GLRT approach respectively. The GLRT receiver, called GLRT2 receiver in the following, assumes an unknown, stationary, Gaussian, spatially colored and temporally white total noise, contrary to the GLRT1 receiver which assumes an unknown, stationary, Gaussian,

spatially and temporally white total noise. The GLRT2 receiver has been shown in [30], by computer simulations and at least for moderate signal to noise ratio (SNR), to be the best receiver for non-orthogonal synchronization sequences. An asymptotical analytical performance analysis of this receiver has been presented recently in [31] and [33] for nominal and large antenna arrays respectively. Nevertheless, the GLRT2 receiver proposed in [30] may be very costly to implement, for large number of antennas in particular, since, for a (M x N) MIMO system, it requires both a (NxN) matrix inversion and an (NxN) or (MxM) determinant computation at each tested sample position. An alternative to this GLRT2 receiver could be the MMSE receiver proposed in [30]. However, although less complex than the GLRT2 receiver, the MMSE receiver is shown in this paper to be sensitive to the synchronization sequences correlations, which may limit its practical use in this case.

In this context, the purpose of this paper is to get new insights into the time synchronization of SC MIMO links, both without and with interference, in order to overcome the limitations of the available receivers. In the absence of interference, the MIMO GLRT1 receiver is computed for arbitrary synchronization sequences and compared, through a unified framework, to most of the receivers of the literature, enlightening its better performance in most cases for non-orthogonal synchronization sequences in particular. In the presence of interference, as the complexity is an important issue for practical implementations, several ways to decrease the complexity of the GLRT2 receiver while keeping its performance are proposed. The first way to decrease the GLRT2 receiver complexity is to introduce two new MIMO receivers which are robust to interference. These two new receivers, called in the following E0-GLRT3 and E1-GLRT3 receivers respectively, correspond to two estimates of the GLRT receiver in known, stationary, Gaussian, spatially correlated and temporally white total noise, called GLRT3 receiver. These new receivers are shown in the paper to be as much powerful as the GLRT2 receiver but with a lower complexity. For stationary interference, the complexity of both the GLRT2 and E0-GLRT3 receivers may be further reduced by computing and inverting at a lower rate, from an observation interval greater than the synchronization sequence length, the data correlation matrix appearing in these receiver expressions. This strategy is shown to weakly degrade the performance of the considered receivers while substantially decreasing their complexities, especially for large values of M and N. Finally, another way to decrease the previous receiver complexity is to optimize the number of transmit antennas used for synchronization for a given value of the number of receive antennas and for given kinds of propagation channels. Note that such a problem has been preliminary investigated in [25-27], [29] in the DS-CDMA context only and in [32] for precoded synchronization schemes. One of the goals is to enlighten the conditions under which it becomes sub-optimal to implement a MIMO receiver with respect to a SIMO receiver [34] [35] for time synchronization. The performance of the proposed optimization schemes and associated receivers, jointly with their complexity, are analyzed in this paper and compared with that of the GLRT2 receiver, enlightening the

practical interest of the former. Note that preliminary results of the paper in the presence of interference have been presented in [36] but without any proof.

The paper is organized as follows. Section 2 introduces the system model and formulates the problem which is addressed in this paper. Section 3 recalls the basics of detection, the likelihood ratio test and the principle of the GLRT. Section 4 assumes an absence of interference, computes the GLRT1 receiver and compares its structure with that of the main receivers of the literature. Section 5 considers the presence of interference and recalls the GLRT2 and MMSE receivers introduced in [30]. Section 6 computes the GLRT3 receiver and introduces two new receivers, the E0-GLRT3 and E1-GLRT3 receivers, robust to interference and derived from the GLRT3 receiver. Section 7 describes how to decrease the computation rate of the estimated correlation matrix appearing in the previous receivers. Section 8 presents a comparative complexity analysis of the considered receivers, enlightening the great interest of the proposed receivers. Section 9 presents a numerical comparative performance analysis of the receivers introduced in sections 4 to 7, without and with interference, for orthogonal and non-orthogonal synchronization sequences and for deterministic and random channels. It also investigates the optimization of the number of transmit antennas for several kinds of propagation channels. Finally Section 10 concludes this paper.

Before proceeding, we fix the notations used throughout the paper. Italic lower (upper) case non boldface symbols denote scalar (matrices) whereas italic lower case boldface symbols denote column vectors. T, H and * means the transpose, conjugate transpose and conjugate, respectively.

2. OBSERVATION MODEL AND PROBLEM FORMULATION

2.1 Hypotheses and observation model

We consider a (MxN) MIMO radiocommunication link with M and N narrow-band antennas at transmission and reception respectively, and we denote by $\boldsymbol{s}(k)$ the (Mx1) synchronization sequence vector transmitted at time k, with components $s_i(k)$, ($1 \leq i \leq M$), known by the receiver. Assuming a flat fading propagation channel and perfect frequency synchronization, the vector, $\boldsymbol{x}(k)$, of the complex envelopes of the signals at the output of the N receive antennas at time k can be written as

$$\boldsymbol{x}(k) = H\,\boldsymbol{s}(k - l_0) + \boldsymbol{v}(k) = \sum_{i=1}^{M} s_i(k - l_0)\,\boldsymbol{h}_i + \boldsymbol{v}(k) \qquad (1)$$

Here, H is the (NxM) channel matrix whose column i is the vector $\boldsymbol{h}_i$, l_0 is the unknown propagation delay between the transmitter and receiver and $\boldsymbol{v}(k)$ is the sampled total noise vector at time k, which contains the potential contribution of MUI interference, jammers and background noise and which is assumed to be uncorrelated with $\boldsymbol{s}(k - l_0)$. Assuming synchronization sequences of lenght K, denoting by $X(l_0)$ and $V(l_0)$ the (NxK) observation and total noise matrices $X(l_0) =^{\Delta} [\boldsymbol{x}(1+ l_0), \boldsymbol{x}(2+ l_0), ..., \boldsymbol{x}(K + l_0)]$ and $V(l_0) =^{\Delta} [\boldsymbol{v}(1+ l_0),$

$\boldsymbol{v}(2+ l_0)$, ..., $\boldsymbol{v}(K + l_0)$] respectively and by S the (M x K) synchronization sequence matrix $S =;^{\Delta}$ [$\boldsymbol{s}(1)$, $\boldsymbol{s}(2)$, ..., $\boldsymbol{s}(K)$], we obtain, from (1)

$$X(l_0) = H S + V(l_0) \quad (2)$$

Note that the flat fading assumption is required here to develop receivers with a limited complexity but is not required in practice where the considered receivers may be used even for frequency selective fading channels, considering multiple paths as interference.

2.2 Problem formulation

The problem of time synchronisation of the MIMO link consists in estimating the unknown delay l_0 from the observations and the knowledge of S. This can be done by searching for the integer l, denoted by $l;^{\wedge}_0$, for which the matrix S is either optimally estimated or optimally detected from the observations, in a given sense. From the latter point of view, considering first the unknown optimal delay l_0, the synchronization problem may be viewed as a detection problem with two hypotheses [30], [35]. The first hypothesis (H_1) is that the matrix S is perfectly aligned in time in the observation matrix $X(l_0)$ and corresponds to model (2). The second hypothesis (H_0) is that there is no signal in the observation matrix $X(l_0)$ and corresponds to model (3) given by

$$X(l_0) = V(l_0) \quad (3)$$

Note that the third hypothesis (H_2) corresponding to a signal matrix which is misaligned in the observation matrices $X(l)$ for $l \neq l_0$ is not taken into account in the detection approach. The first reason is that a detection test with three hypotheses is much more difficult to implement than a detection test with two hypotheses. The second reason is that the time synchronization problem, viewed as an estimation problem of the SOI time delay from a set of observation vectors, generate estimators which are equivalent, under some assumptions, to detectors built from a two hypothesis detection approach. Such an equivalence has been shown in the literature for SIMO systems where an MMSE approach for SOI or delay estimation [34] has been shown to be equivalent to a GLRT detection approach [35] for time synchronization purposes.

The two hypotheses detection problem of matrix S from $X(l_0)$ then consists in elaborating a statistical test, $C(l_0)$, function of $X(l_0)$, and to compare the value of this test to a threshold. The detection is considered if the threshold is exceeded. As in practice l_0 is unknown, the problem is to estimate it by computing $C(l)$ for arbitrary values of l around l_0 and to select the value of l which maximizes $C(l)$ under the constraint of exceeding the threshold. For synchronization sequences with perfect autocorrelation properties, the latter processing would be sufficient. However in practice, the synchronization sequences have imperfect autocorrelation properties and the misaligned case, which is not taken into account in the theoretical approach, may also generate a detection (due to the ambiguity functions of the sequences). For this reason, to prevent false detection of the signal, we use to test several time positions around a tested position which has generated a

detection. More precisely, whenever a tested position l generates a detection (i.e. $C(l)$ is greater than or equal to the threshold), to within a false alarm, it may be generated either by an aligned or by a misaligned signal. To remove the detection of the misaligned signals, we compute and compare to the threshold $C(l+k)$ for $-K \leq k \leq K$, where K is the sequence length. Among the values $l+k$ such that $C(l+k)$ is above the threshold, the best estimate, $\hat{l}_0$, of l_0 corresponds to the delay $l+k$ which maximizes $C(l+k)$.

As the main purpose of the paper is to compare several statistical tests for synchronization, to simplify the notations, we consider in the following the generic detection problem of the (M x K) matrix S from the (N x K) observation matrix X with two hypotheses H_1 and H_0. Under H_1, S is perfectly aligned in time with X whereas under H_0, there is no matrix S in X which corresponds to the (N x K) total noise matrix V and we obtain:

$$H_1: \; X = H S + V \tag{4a}$$

$$H_0: \; X = V \tag{4b}$$

where $X \overset{\Delta}{=} [\boldsymbol{x}(1), \boldsymbol{x}(2), ..., \boldsymbol{x}(K)]$ and $V \overset{\Delta}{=} [\boldsymbol{v}(1), \boldsymbol{v}(2), ..., \boldsymbol{v}(K)]$ respectively. The problem addressed in this paper is to introduce different statistical tests for the detection of matrix S, built from different approaches and/or different hypotheses, and to compare them with those of the literature from both a complexity and a performance point of view. The performance of a statistical test is characterized by the probability of a good detection of S, i.e that the statistical test exceeds the threshold, under H_1 (P_D), for a given false alarm probability (P_{FA}), corresponding to the probability to exceed the threshold under H_0. The performance comparison of the different statistical tests will be done without and with interference, for different channel matrix H (deterministic or random), synchronization sequences (orthogonal or not) and number of antennas (small or high). The possibility of a computation rate decrease of the correlation matrix of the observations is also investigated. Finally the number of transmit antennas for synchronization is optimized for different scenarios of channel matrix and number of receive antennas.

3. THE LRT RECEIVER AND GLRT PRINCIPLE

According to the Neyman-Pearson theory of detection [37], the optimal statistical test for the detection of matrix S from matrix X is the LRT, which consists in comparing the function $LRT \overset{\Delta}{=} p[X/ H_1] / p[X/ H_0]$ to a threshold, where $p[X/ H_i]$ ($i = 0, 1$), is the conditional probability density of X under H_i. To compute this statistical test, we assume that the sampled vectors $\boldsymbol{v}(k)$ are zero-mean, stationary, independent and identically distributed (i.i.d), temporally white, circular and Gaussian with covariance matrix $R \overset{\Delta}{=} E[\boldsymbol{v}(k) \, \boldsymbol{v}(k)^H]$. Under these assumptions and using (4), the LRT takes the form:

$$\text{LRT} = \prod_{k=1}^{K} \frac{p_{H_1}[\boldsymbol{x}(k) / \boldsymbol{s}(k), H, R]}{p_{H_0}[\boldsymbol{x}(k) / R]} \gtrless_{H_0}^{H_1} \eta_1 \quad (5)$$

where $p_{H_1}[\boldsymbol{x}(k) / \boldsymbol{s}(k), H, R]$ and $p_{H_0}[\boldsymbol{x}(k) / R]$ are given by

$$p_{H_1}[\boldsymbol{x}(k) / \boldsymbol{s}(k), H, R] \overset{\Delta}{=} \pi^{-N} \det[R]^{-1} \exp[-(\boldsymbol{x}(k) - H\,\boldsymbol{s}(k))^{H} R^{-1} (\boldsymbol{x}(k) - H\,\boldsymbol{s}(k))] \quad (6)$$

$$p_{H_0}[\boldsymbol{x}(k) / R] \overset{\Delta}{=} \pi^{-N} \det[R]^{-1} \exp[-\boldsymbol{x}(k)^{H} R^{-1} \boldsymbol{x}(k)] \quad (7)$$

where $\det[R]$ means determinant of R. In the absence of interference, vectors $\boldsymbol{v}(k)$ are assumed to be spatially white such that $R = \eta_2 I_N$, where η_2 is the mean power of the noise per receive antenna and I_N is the identity matrix of dimension N. In this case, the LRT, denoted by LRT1, takes the form:

$$\text{LRT1} = \prod_{k=1}^{K} \frac{p_{H_1}[\boldsymbol{x}(k) / \boldsymbol{s}(k), H, \eta_2]}{p_{H_0}[\boldsymbol{x}(k) / \eta_2]} \gtrless_{H_0}^{H_1} \eta_1 \quad (8)$$

where $p_{H_1}[\boldsymbol{x}(k) / \boldsymbol{s}(k), H, \eta_2]$ and $p_{H_0}[\boldsymbol{x}(k) / \eta_2]$ are given by (6) and (7) respectively with $R = \eta_2 I_N$. However, as in practice (η_2, H), in the absence of interference, or (R , H), in the presence of interference, are unknown, they have to be replaced in (8) and (5) respectively by their maximum likelihood (ML) estimates under H_1 (for H) and under H_1 and H_0 (for η_2 or R), giving rise to the GLRT1 and GLRT2 respectively, presented in the following sections. Nevertheless, note that GLRT detectors are no longer LRT detectors and then become sub-optimal detectors.

4. TIME SYNCHRONIZATION WITHOUT INTERFERENCE

In this section, we compute the GLRT1 receiver for time synchronization in the absence of interference for arbitrary synchronization sequences. The structure of this receiver is then compared, through a unified framework, with that of the main receivers of the literature in the absence of interference, which is original. A comparative performance analysis of these receivers, also original, is then presented in section 9, enlightening,

for not too small SNR, the better performance of the GLRT1 receiver for non-orthogonal synchronization sequences in particular.

4.1 GLRT1 receiver

Replacing in (8) η_2 and H by their ML estimates under H_1 (for H) and under H_1 and H_0 (for η_2), it is shown in Appendix A that a sufficient statistic for the GLRT1 is given by

$$\text{GLRT1} = \frac{\text{Tr}(\hat{R}_{xs} R_s^{-1} \hat{R}_{xs}^H)}{\text{Tr}(\hat{R}_x)} \tag{9}$$

where Tr(.) means Trace and where matrices $\hat{R}_x$, R_s and $\hat{R}_{xs}$ are defined by

$$\hat{R}_x \triangleq XX^H / K = \frac{1}{K} \sum_{k=1}^{K} \boldsymbol{x}(k)\, \boldsymbol{x}(k)^H \quad ; \quad R_s \triangleq SS^H / K = \frac{1}{K} \sum_{k=1}^{K} \boldsymbol{s}(k)\, \boldsymbol{s}(k)^H \tag{10}$$

$$\hat{R}_{xs} \triangleq XS^H / K = \frac{1}{K} \sum_{k=1}^{K} \boldsymbol{x}(k)\, \boldsymbol{s}(k)^H \triangleq [\hat{\boldsymbol{r}}_{xs_1}, \ldots, \hat{\boldsymbol{r}}_{xs_M}] \tag{11}$$

with

$$\hat{\boldsymbol{r}}_{xs_i} \triangleq \frac{1}{K} \sum_{k=1}^{K} \boldsymbol{x}(k)\, s_i(k)^* \quad ; \quad \text{Tr}(\hat{R}_x) = \frac{1}{K} \sum_{k=1}^{K} \boldsymbol{x}(k)^H \boldsymbol{x}(k) \triangleq \hat{r}_x \tag{12}$$

Note that the element $[i, j]$, $R_s[i, j]$, $(1 \leq i, j \leq M)$ of R_s corresponds to the correlation of the synchronization sequences i and j. Thus, $R_s[i, i]$, denoted in the following by r_{si}, is the mean power of the sequence i. Expression (9), which does not seem to be published in the literature, requires that R_s is invertible, which is only possible if $M \leq K$ and which is assumed in the following. Note that this condition does not prevent M to be large, provided that K is at least as large as M.

In the particular case of M orthogonal synchronization sequences, expression (9) reduces to

$$\text{GLRT1} = \sum_{i=1}^{M} \frac{\hat{\boldsymbol{r}}_{xs_i}^H \hat{\boldsymbol{r}}_{xs_i}}{\hat{r}_x\, r_{si}} \tag{13}$$

which corresponds to the sum of M SIMO GLRT1 statistics, each one being associated with a transmitted antenna.

4.2 Receivers of the literature

Several statistical tests for time synchronization of MIMO links in the absence of interference have been proposed in the literature [10-15], [17-27], [29], mainly for DS-CDMA and OFDM links. Some of them may be also used for non DS-CDMA SC links. It is then interesting and important in practice to compare the most popular ones with the GLRT1 through a unified framework.

a) *Mody's Test*

One of the reference test for time synchronization of MIMO links without interference is the one proposed in [10], [13] for OFDM links. It assumes orthogonal training sequences such that $\boldsymbol{s}(k)^{H}\boldsymbol{s}(k) = 1$, $1 \le k \le K$, and may also be used for SC links. It can be written as

$$\text{Mody} \underset{\Delta}{=} \underset{j}{\text{Sup}} \left\{ \sum_{i=1}^{M} \frac{\left| \hat{r}_{xjs_i} \right|^2}{\hat{r}_{xj}} \right\} \tag{14}$$

where $\hat{r}_{xjs_i}$ and $\hat{r}_{xj}$ are defined by the first and second part of (12) respectively with $x_j(k)$ replacing $\boldsymbol{x}(k)$.

b) *Correlation test*

Another reference test for time synchronization of MIMO links without interference is the correlation test proposed in [30] for SC links. It makes no assumptions on the synchronization sequences. It can be written as:

$$\text{COR} \underset{\Delta}{=} \sum_{i=1}^{M} \frac{\hat{\boldsymbol{r}}_{xs_i}^{H} \hat{\boldsymbol{r}}_{xs_i}}{\hat{r}_x \left[\sum_{m=1}^{M} r_{sm} \right]} \tag{15}$$

c) *Least square MIMO channel estimate test*

An alternative to the correlation test is the least square (LS) MIMO channel estimate test proposed in [30], called hereafter LS test, which still makes no assumptions on the synchronization sequences. It consists in comparing to a threshold the normalized Frobenius norm squared of the (NxM) LS channel estimate $\hat{H} \underset{\Delta}{=} \hat{R}_{xs} R_s^{-1}$. We then deduce that the LS test can then be written as:

$$\text{LS} \underset{\Delta}{=} \frac{\text{Tr}[\hat{R}_{xs} \hat{R}_s^{-2} \hat{R}_{xs}^{H}]}{\hat{r}_x \, \text{Tr}[R_s^{-1}]} \tag{16}$$

In the particular case of M orthogonal synchronization sequences, expression (16) reduces to

$$LS = \sum_{i=1}^{M} \frac{r_{si}^{-2}\, \boldsymbol{r}_{xs_i}^{H}\, \boldsymbol{r}_{xs_i}}{r_x \left[\sum_{m=1}^{M} r_{sm}^{-1}\right]} \qquad (17)$$

d) *Synthesis*

We deduce from the previous expressions, in the absence of interference, that for orthogonal synchronization sequences having the same power, the COR and the LS tests, for a (*M*x*N*) MIMO link, and the Mody's test, for a (*M*x1) MISO link, are equivalent to the GLRT1. This allows us to obtain, in this case, alternative interpretations of the GLRT1 receiver. Otherwise, and for non-orthogonal sequences in particular, the Mody's, COR and LS tests are no longer equivalent to the GLRT1 which may expect to give better results than the others as it will be analyzed in section 9.

5. RECEIVERS IN THE LITERATURE FOR TIME SYNCRONIZATION WITH INTERFERENCE

In this section, we briefly recall the GLRT2 and MMSE receivers introduced in [30] for time synchronization in the presence of interference.

5.1 GLRT2 receiver

In the presence of interference, the total noise $\boldsymbol{v}(k)$ is spatially colored and R is no longer proportional to the identity matrix. Replacing in (5) H by its ML estimate under H_1 and R by its ML estimate under both H_1 and H_0, it has been shown in [30] that a sufficient statistic for the GLRT2 is given by

$$GLRT2 = \det[I_K - P_s \hat{P}_x]^{-K} \qquad (18)$$

where det[.] means determinant and where P_S and $\hat{P}_x$ are (*K*x*K*) matrices corresponding to the orthogonal projectors onto the row spaces of S and X respectively, defined by $P_S \overset{\Delta}{=} S^H(SS^H)^{-1}S$ and $\hat{P}_x \overset{\Delta}{=} X^H(XX^H)^{-1}X$. Using properties of the determinant, it is straighforward to show that (18) can also be written as

$$GLRT2 = \det[I_N - \hat{R}_x^{-1}\hat{R}_{xs} R_s^{-1} \hat{R}_{xs}^{H}]^{-K} = \det[I_M - R_s^{-1}\hat{R}_{xs}^{H}\hat{R}_x^{-1}\hat{R}_{xs}]^{-K} \qquad (19)$$

Note that (19), less costly than (18) when $K > \mathrm{Max}(N, M)$, has not been presented in [30]. For time synchronization, expressions (18) and (19) show that, at each tested sample position, the GLRT2 receiver requires the computation of at least a (*N*x*N*) matrix inversion, $\hat{R}_x^{-1}$, and the determinant of a (*P*x*P*) matrix where $P = \mathrm{Min}(K, N, M)$, which may be prohibitive for large K and large values of the number of antennas.

In the particular case of a SIMO system ($M = 1$), the vector $\boldsymbol{s}(k)$ reduces to the scalar $s_1(k)$, the matrix $\hat{R}_{xs}$ reduces to the vector $\hat{\boldsymbol{r}}_{xs_1}$, R_S reduces to the scalar r_{s_1} and we deduce from (19) that a sufficient statistic for the GLRT2 is given by

$$\mathrm{GLRT2}_{SIMO} = \frac{\boldsymbol{r}_{xs_1}^{H} R_x^{-1} \boldsymbol{r}_{xs_1}}{r_{s1}} \tag{20}$$

result already obtained in [34] and [35].

5.2 MMSE receiver

Time synchronization from the MMSE receiver consists in finding the sample position which minimizes the LS error, ε, between the known sampled vectors $\boldsymbol{s}(k)$ and their LS estimation from a spatial filtering of the data $\boldsymbol{x}(k)$ ($1 \le k \le K$). After elementary computations, it can be verified that a sufficient statistic for the MMSE receiver is given by [30]

$$\mathrm{MMSE} \quad =^{\Delta} \quad \frac{\mathrm{Tr}(R_{xs}^{H} R_x^{-1} R_{xs})}{\mathrm{Tr}(R_s)} = \sum_{i=1}^{M} \frac{\boldsymbol{r}_{xs_i}^{H} R_x^{-1} \boldsymbol{r}_{xs_i}}{[\sum_{m=1}^{M} r_{sm}]} \tag{21}$$

Comparing (21) to (20), we deduce that, to within a constant, the MMSE receiver corresponds to the weighted sum of M SIMO receivers, each of them being associated with a particular transmit antenna. The computation of the MMSE receiver requires a (NxN) matrix inversion at each tested sample position but no determinant computation, which is less complex than the GLRT2 computation. For SIMO links (M = 1), (21) reduces to (20) and the MMSE and GLRT2 receivers coincide. However for MIMO links (M > 1), this result is a priori no longer true, even for orthogonal synchronization sequences having the same power, and this result is still valid for $M \ge 2$, which was not obvious a priori. Thus, despite its lower complexity, the MMSE receiver is potentially less powerful than the GLRT2 receiver, as shown in [30] for non-orthogonal sequences and moderate SNR in particular. This motivates the development of alternative receivers aiming at improving the performance of the MMSE receiver, and at approaching the performance of the GLRT2 receiver, whatever the orthogonality of the synchonization sequences, which is the purpose of the next section.

6. NEW RECEIVERS FOR TIME SYNCRONIZATION WITH INTERFERENCE

The direct computation of the determinant (19) is not so straitghtforward for M > 2 while the MMSE receiver (21) has been shown in [30] to become sub-optimal for non-orthogonal synchronization sequences at not too low SNR. In this context, a way to decrease the complexity of the GLRT2 receiver for arbitrary values of M while trying to keep its performance is to develop new alternative receivers. To this aim, it seems natural to think that non-GLRT receivers corresponding to good estimates of the GLRT receiver in known total noise, called

GLRT3 receiver, have good chances to approach the performance of the GLRT2 receiver. For this reason, in this section, we introduce the GLRT3 receiver and we propose two new receivers corresponding to two different estimates of the GLRT3 receiver.

6.1 GLRT3 receiver

The GLRT3 receiver is obtained by considering expression (5), assuming an unknown channel matrix H and a zero-mean, i.i.d stationary, circular, Gaussian total noise whose covariance matrix, R, is assumed to be known. Replacing in (5) H by its ML estimate, $\hat{H} = \hat{R}_{xs} R_s^{-1}$, generates the GLRT3 receiver. It is shown in Appendix B that a sufficient statistic for the GLRT3 receiver is given by

$$\text{GLRT3} = \text{Tr}(R_s^{-1} \hat{R}_{xs}^{\text{H}} R^{-1} \hat{R}_{xs}) \tag{22}$$

In the particular case of M orthogonal synchronization sequences, expression (22) reduces to

$$\text{GLRT3} \stackrel{\Delta}{=} \sum_{i=1}^{M} \frac{\boldsymbol{r}_{xs_i}^{\text{H}} R^{-1} \boldsymbol{r}_{xs_i}}{r_{si}}$$

(23)

Expressions (22) and (23) show that the GLRT3 receiver does not require any determinant computation and corresponds, for orthogonal sequences, to the sum of M SIMO GLRT3 receivers, each one being associated with a transmitting antenna. Unfortunately, it cannot be used in pratice since R is unknown but it can be estimated by replacing R by an estimate $\hat{R}$, which is done in the following sections.

6.2 Estimated GLRT3 receiver under H0

A first possibility to built from (22) a new receiver useful in practice is to replace in (22) the matrix R by its ML estimate, $\hat{R}_0$, under H0. It is well-known [35] that $\hat{R}_0 = \hat{R}_x$, which gives rise to the estimated GLRT3 receiver under H0 (E0-GLRT3), defined by

$$\text{E0-GLRT3} = \text{Tr}(R_s^{-1} \hat{R}_{xs}^{\text{H}} \hat{R}_x^{-1} \hat{R}_{xs})$$

(24)

In the particular case of M orthogonal synchronization sequences, expression (24) reduces to

$$\text{E0-GLRT3} \stackrel{\Delta}{=} \sum_{i=1}^{M} \frac{\boldsymbol{r}_{xs_i}^{\text{H}} \hat{R}_x^{-1} \boldsymbol{r}_{xs_i}}{r_{si}} \tag{25}$$

which corresponds, to within a constant and for orthogonal sequences having the same power, to the MMSE statistical test defined by (21). This gives, in this case, an interpretation of the MMSE receiver in terms of estimate of the GLRT3 receiver under H0. Otherwise, E0-GLRT3 receiver has no link with the MMSE receiver.

6.3 Estimated GLRT3 receiver under H1

A second possibility to built from (22) a new receiver useful in practice is to replace in (22) the matrix R by its ML estimate, $\hat{R}_1$, under H1. It is well-known that $\hat{R}_1$ is defined by [23], [35]

$$\hat{R}_1 = \hat{R}_x - \hat{R}_{xs} R_s^{-1} \hat{R}_{xs}^H \quad (26)$$

In (26) the estimated contributions of the transmitted synchronization sequences have been removed from $\hat{R}_x$. This gives rise to the estimated GLRT3 receiver under H_1 (E1-GLRT3), defined by

$$\text{E1-GLRT3} = \text{Tr}(R_s^{-1} \hat{R}_{xs}^H \hat{R}_1^{-1} \hat{R}_{xs}) \quad (27)$$

In the particular case of M orthogonal synchronization sequences, expression (27) reduces to

$$\text{E1-GLRT3} \triangleq \sum_{i=1}^{M} \frac{\boldsymbol{r}_{xs_i}^H \hat{R}_1^{-1} \boldsymbol{r}_{xs_i}}{r_{si}} \quad (28)$$

7. COMPUTATION RATE DECREASE OF $\hat{R}_x$

In practice, at each tested sample position l, the computation of $C(l)$ from the GLRT2, MMSE, E0-GLRT3 and E1-GLRT3 receivers requires the computation of both a new (NxN) correlation matrix $\hat{R}_x(l) \triangleq X(l)X(l)^H / K$, over K observation samples, and a new (NxN) matrix inversion ($\hat{R}_x(l)^{-1}$ or $\hat{R}_1(l)^{-1}$). This generates a computation rate of one $\hat{R}_x(l)$ matrix plus one matrix inverse per time sample l, which may become very costly for high values of N. In particular, for samples l generating a detection, we have to test $2K+1$ positions around l (C($l+k$) for $-K \leq k \leq K$), which means that we have to compute and to invert $2K+1$ correlation matrix estimates $\hat{R}_x(l+k)$, $-K \leq k \leq K$.

In this context, an additional way to decrease the complexity of the GLRT2 and E0-GLRT3 receivers is to decrease the computation rate of $\hat{R}_x(l)$ and $\hat{R}_x(l)^{-1}$ by a factor $\beta > 1$. More precisely, the principle is to built an (NxK') observation matrix $X'(l) = [\boldsymbol{x}(1+l), \boldsymbol{x}(2+l), ..., \boldsymbol{x}(K'+l)]$ from K' observation samples instead of K, such that $K' > K$, to replace $\hat{R}_x(l) \triangleq X(l)X(l)^H / K$ by $\hat{R}_{x'}(l) \triangleq X'(l)X'(l)^H / K'$, and to use the same correlation matrix estimate, $\hat{R}_{x'}(l)$ (instead of $\hat{R}_x(l)$), for the $\beta = K' - K + 1$ tested position $l + i$ ($0 \leq i \leq \beta - 1$). Using this strategy in the GLRT2 and E0-GLRT3 receivers gives rise to GLRT2-CRD and E0-GLRT3-CRD receivers respectively, where R-CRD means receiver R with a computation rate decrease. Note that $K' - K$ samples are now data samples instead of synchronization samples. As the data samples associated with different antennas are uncorrelated, this strategy to decrease the complexity of GLRT2 and E0-GLRT3 receivers is only valid for orthogonal synchronization sequences. Of course, this strategy requires constant values of H and R

over K' samples, which may limit the value of K'. However, it allows to compute and to inverse only one (NxN) matrix per set of β tested sample positions, hence a gain of β in the matrix computation and inversion. Note that this strategy cannot be applied to the E1-GLRT3 receiver since the computation of $\hat{R}_1$ from (26) and thus its inversion, requires an update of $\hat{R}_{xs}$ at each time samples.

8. COMPLEXITY ANALYSIS

In order to get more insights into the relative complexities of the receivers which are robust to interference, we present in this section a complexity analysis of the latter. Note that the complexity of a receiver corresponds to the approximate number of complex operations required to compute the associated statistical test. Note that complexity analysis through big-O(var) notation has full meaning when var is high. For small values of var, the meaning of big-O notations decreases and a more detailed analysis, which uses assumptions of section 8.1, is required.

8.1 Assumptions

To compute the complexity of a receiver, we need to briefly recall the complexity of some common operations on a (NxN) matrix A.

- The cost of the LU decomposition of A is approximately $2N^3/3$.

- Using the LU decomposition of A, we easily deduce that the complexity of the determinant computation of A is $2N^3/3 + 2(N-1) + 1$.

- Using the LU decomposition of A, the total cost required to inverse A is $2N^3/3 + 2N^3 = 8N^3/3$.

- The cost of a matrix $C = EB$, where E is a (NxK) matrix and B is a (KxM) matrix is $NM(2K-1)$. If E and B are both (NxN), the cost is $N^2(2N-1) = 2N^3 - N^2$. In the particular case where $C = EE^{\mathrm{H}}$, the matrix C is Hermitian and the cost becomes $(N^2+N)(2K-1)/2$.

8.2 Complexity analysis

Since the receivers with computation rate decrease are only applicable for orthogonal synchronization sequences, we assume here that the sequences are orthogonal, i.e. that R_s is diagonal. Moreover, as in practice the sequences have equal power, we assume that R_s is proportional to identity and that the sequences are normalized in power. Under these assumptions, as the MMSE and E0-GLRT3 receivers are equivalent, we only consider GLRT2, GLRT2-CRD, E0-GLRT3 and E0-GLRT3-CRD receivers. Moreover, by defining $G_N \overset{\Delta}{=} \hat{R}_x^{-1}\hat{R}_{xs}\hat{R}_{xs}^{\mathrm{H}}$ and $G_M \overset{\Delta}{=} \hat{R}_{xs}^{\mathrm{H}}\hat{R}_x^{-1}\hat{R}_{xs}$, we deduce from (19) and (24) that the GLRT2 and E0-GLRT3 receivers can be rewritten as

$$\text{GLRT2} = \det[\mathrm{I}_N - G_N]^{-K} = \det[\mathrm{I}_M - G_M]^{-K} \tag{29}$$

$$\text{E0-GLRT3} = \mathrm{Tr}(G_M) = \mathrm{Tr}(G_N) \tag{30}$$

Thus, the computation of both statistics requires the computation of either G_N or G_M. In practice, to minimize the complexity, we may choose to compute GP where $P = \text{Min}(N, M)$. In the following we choose to compute G_M. Under these assumptions, Table 1 indicates the number of operations required to compute each receiver using G_M. Moreover, Figure 1 shows, for $K = 32$, $K'/K = 10$, $M = 2$ and $M = 8$, the number of complex operations required to compute the GLRT2, GLRT2-CRD, E0-GLRT3 and E0-GLRT3-CRD receivers as a function of N. Note the increasing complexity with M and N for all the receivers. Note, from a complexity point of view, the increasing interest of E0-GLRT3 with respect to GLRT2 as M increases. Note the increasing interest of E0-GLRT3-CRD and GLRT2-CRD with respect to E0-GLRT3 and GLRT2 as M increases. Note finally the great interest to optimize the value of M at least from a complexity point of view.

Table 1

Figure 1

9. SIMULATIONS AND DISCUSSIONS

We present in this section a comparative performance analysis of most of the MIMO receivers introduced in sections 4 to 7. These receivers are first compared without interference and then with interference. This analysis allows us in particular to enlighten the practical interest of the new receivers introduced in this paper (GLRT1, E0-GLRT3, E1-GLRT3, GLRT2-CRD, E0-GLRT3-CRD) with respect to the receivers of the literature and to the GLRT2 receiver in particular, which has been considered to be the best receiver in [30] at least for non-orthogonal sequences and not too low SNR. Finally, the optimization of the number of transmit antennas, M, for several kinds of propagation channel matrix H, is investigated at the end of the section.

9.1 Assumptions

a) *Array of antennas*

We consider in this section 9 (MxN) MIMO links for which the transmitting and the receiving antennas are omnidirectional. The receiving array of antennas is a uniform linear array of N antennas spaced half a wavelenght apart, whereas the geometry of the transmitting array may be arbitrary, depending of the scenario.

b) *Channel matrix*

Two kinds of channel matrix H, corresponding to deterministic and random channel matrices, are considered. In the deterministic case, which may correspond to a line of sight (LOS) situation, the transmitted antennas are assumed to be potentially distributed in space or well-separated from each other, the channel is assumed to be a free space propagation channel and the channel vectors $\boldsymbol{h}_i$ correspond, to within a phase term, to steering vectors for the receiving array. In this case, the vector $\boldsymbol{h}_i$ is defined by $\boldsymbol{h}_i =;^{\Delta} \exp(j\phi_i)$ $[1, \exp(j\pi\sin(\theta_i)),\exp(j2\pi\sin(\theta_i)),....,\exp(j(N-1)\pi\sin(\theta_i))]^T$, where θ_i is the angle of arrival (AOA) of sequence i with respect to broadside, whereas ϕ_i corresponds to a phase term, function of the transmitting array geometry.

The colinearity degree of the channel vectors $\boldsymbol{h}_i$ and $\boldsymbol{h}_j$ is characterized by the spatial correlation coefficient, α_{ij} ($1 \leq i,j \leq M$), between $\boldsymbol{h}_i$ and $\boldsymbol{h}_j$, such that $0 \leq |\alpha_{ij}| \leq 1$ and defined by

$$\alpha_{ij} =;^{\Delta} \frac{\boldsymbol{h}_i^{\dagger}\boldsymbol{h}_j}{(\boldsymbol{h}_i^{\dagger}\boldsymbol{h}_i)^{1/2}(\boldsymbol{h}_j^{\dagger}\boldsymbol{h}_j)^{1/2}}; \qquad (31)$$

In the random case, the transmitted antennas are no longer distributed in space and the coefficients, H_{ij}, of the channel matrix H are assumed to be zero-mean i.i.d, circular and Gaussian variables such that $E[|H_{ij}|^2] = 1$, which modelizes a Rayleigh flat fading channel with a maximal diversity.

c) *Synchronization sequences*

Each synchronization sequence is composed of K samples. These sequences have the same power ($r_{si} =;^{\Delta} r_s$, $1 \leq i \leq M$) and are normalized such that the signal to thermal noise ratio per receive antenna, defined by $SNR =;^{\Delta} M\, r_s / \eta_2$, may be arbitrary chosen.

Orthogonal sequences correspond to cyclically shifted Zadoff-Chu sequences [38]. More specifically, the rows of matrix S are chosen as cyclic shifts of a Zadoff-Chu sequence of length K, such that $R_s = r_s\, I_M$.

Non-orthogonal sequences are composed of quadrature phase shift keying (QPSK) complex symbols. The correlation degree of two sequences i and j is characterized by the temporal correlation coefficient, ρ_{ij} ($1 \leq i,j \leq M$), such that $0 \leq |\rho_{ij}| \leq 1$ and defined by

$$\rho_{ij} =;^{\Delta} \frac{r_{sij}}{(r_{si})^{1/2}(r_{sj})^{1/2}}; \qquad (32)$$

where $r_{sij} =;^{\Delta} R_s[i, j]$. The sequences i and j are orthogonal if $\rho_{ij} = 0$. In practice, the correlation value between sequences is obtained by splitting each antennas sequence in two subsequences. The first subsequence is composed of the same QPSK symbols for every antenna, whereas the second subsequences are independent and random QPSK symbols. By changing the first subsequence length with respect to K, we obtain different correlation values. In the following $K = 32$.

d) *Total noise model*

Over a duration interval on which the channel does not change, the total noise vector $\boldsymbol{v}(k)$ is assumed to be composed of one rank-one single antenna interference, whose associated channel vector has no delay spread, and a background noise and can be written as

$$\boldsymbol{v}(k) = j_I(k)\, \boldsymbol{h}_I + \boldsymbol{n}(k) \qquad (33)$$

Here, $\boldsymbol{n}(k)$ is the sampled background noise vector, assumed to be zero-mean, stationary, Gaussian, SO circular, spatially and temporally white with a mean power per received antenna equal to η_2, $j_I(k)$ is the complex sample at time k of the interference, such that $\pi_I =;^{\Delta} E[|j_I(k)|^2]$ is the input mean power of the interference per antenna. In the following, $j_I(k)$ is either a QPSK interference sampled at the symbol rate or a stationary, circular complex Gaussian interference whose samples are i.i.d. Vector $\boldsymbol{h}_I$, with components $\boldsymbol{h}_I[i]$ ($1 \leq i \leq N$), is the channel vector of the interference such that the components $\boldsymbol{h}_I[i]$ are either deterministic or random. In the first case, $\boldsymbol{h}_I$ is a steering vector, as discussed in section 9.1 b), whereas in the second case, the components $\boldsymbol{h}_I[i]$ ($1 \leq i \leq N$), are realizations of a zero-mean i.i.d circular Gaussian variables such that $E[|\boldsymbol{h}_I[i]|^2] = 1$. In both cases, over a duration interval on which the channel does not change, R can be written as

$$R = \pi_I \boldsymbol{h}_I \boldsymbol{h}_I^H + \eta_2 I \tag{34}$$

Note that in the simulations, $\boldsymbol{h}_I$ will change for each realization. The interference to noise ratio per receive antenna is defined by $INR =;^{\Delta} \pi_I / \eta_2$. In the absence of interference, INR = 0, whereas in the presence of interference, INR may be such that INR/SNR = 5 or 15 dB. In the following, the false alarm rate is such that $P_{FA} = 10^{-3}$ for all the scenarios. The Figures are built from 10^6 independent realizations.

9.2 Absence of interference

We assume in this section no interference, and we consider both orthogonal and non-orthogonal synchronization sequences.

a) *Orthogonal synchronization sequences*

For orthogonal sequences having the same power, the statistical tests COR and LS are equivalent to GLRT1, whereas MMSE and E0-GLRT3 are equivalent. We thus only consider in this case, GLRT1, Mody, GLRT2, E0-GLRT3 and E1-GLRT3 receivers. Under the previous assumptions, Figures 2a and 2b show, for a (2x2) MIMO link, the variations of the missprobability ($P_M =;^{\Delta} 1 - P_D$) as a function of the SNR per receive antenna at the output of the previous receivers for a deterministic channel matrix H. The vector $\boldsymbol{h}_1$ is associated with an AOA, $\theta_1 = 0°$, which is orthogonal to the line array, whereas $\boldsymbol{h}_2$ corresponds to an AOA θ_2 such $\alpha_{12} = 0$ (2a) and $|\alpha_{12}|^2 = 0.6$ (2b) respectively. Figures 3a and 3b show the same variations but for a random channel matrix H of dimension (2x2) (3a) and (4x4) (3b). For deterministic channels, the increase of $|\alpha_{12}|$ does not alter the performance of the GLRT1 and Mody receivers, while it degrades slightly the GLRT2, E0-GLRT3 and E1-GLRT3 receivers which stay always equivalent. Note the best behaviour of GLRT1 with respect to other receivers and GLRT2 in particular, and the worst behaviour of Mody's receiver in all cases. For random channels, the performance of all the receivers increases from figure (3a) to figure (3b) due to an increase of both receive array gain and transmit and receive spatial diversity. Again, the GLRT1 has the best performance, Mody's receiver has the worst performance and GLRT2, E0-GLRT3 and E1-GLRT3 are almost equivalent.

Figure 2

Figure 3

b) *Non-orthogonal synchronization sequences*

For non-orthogonal sequences, we consider GLRT1, Mody, COR, GLRT2, MMSE, E0-GLRT3 and E1-GLRT3 receivers which are a priori not equivalent. Under these assumptions, Figures 4 and 5 consider the same scenarios and show the same variations as Figures 2 and 3 respectively but for the previous receivers and for non-orthogonal synchronization sequences such that $0.6 \leq |\rho_{ij}| \leq 0.9$. For deterministic channels, the increase of $|\alpha_{12}|$ seems to increase the performance of each receiver. However, whatever the value of $|\alpha_{12}|$, the best receiver is the COR receiver, and does no longer correspond to the GLRT1, which is less powerful than the MMSE and COR receiver but which is more powerful than GLRT2, E0-GLRT3 and E1-GLRT3 which are approximately equivalent. Finally the Mody receiver is still the worse receiver. For random channels, the performance of all the receivers increases from figure (5a) to Figure (5b) due to an increase of both receive array gain and transmit and receive spatial diversity. Moreover, below a certain value of SNR, increasing with the number of antennas, the COR receiver still has the best performance, followed by the MMSE and the GLRT1 receivers. This result has not been presented in [30] which does not consider low SNR. However, above this value of SNR, the GLRT1 becomes the best receiver, followed by the GLRT2, E1-GLRT3 and E0-GLRT3 which are almost equivalent, themselves followed by the COR, MMSE and Mody receivers. Note in this case, a strong performance degradation of the MMSE receiver with respect to the GLRT2, as already found in [30]. Note also, for high SNR, that performance of GLRT2 are not far from that of GLRT1, with a difference which decreases as the number of antennas decreases.

Figure 4

Figure 5

9.3 Presence of interference

We assume in this section the presence of one interference, and we consider both orthogonal and non-orthogonal synchronization sequences.

a) *Orthogonal synchronization sequences*

For orthogonal sequences having the same power, MMSE and E0-GLRT3 are equivalent and thus we only consider in this case, for the robust receivers, GLRT2, E0-GLRT3 and E1-GLRT3 receivers. In addition we also consider GLRT1 and Mody non robust receivers as reference receivers. Under the previous assumptions, Figures 6, 7, on one hand, and Figures 8, 9, on the other hand, consider the same scenarios and show the same variations as Figures 2 and 3 respectively but in the presence of one interference. For Figures 6 and 7, the vector $\boldsymbol{h}_I$ is associated with the DOA $\theta_I = 20°$, which means that $(|\alpha_{12}|^2, |\alpha_{1I}|^2, |\alpha_{2I}|^2) = (0, 0.74, 0.001)$ for Figures 6a and 7a, and $(|\alpha_{12}|^2, |\alpha_{1I}|^2, |\alpha_{2I}|^2) = (0.6, 0.74, 0.97)$ for Figures 6b and 7b, where α_{iI} $(1 \leq i \leq 2)$ is defined by (31) with $\boldsymbol{h}_I$ instead of $\boldsymbol{h}_j$. For figures 8 and 9, $\boldsymbol{h}_I$ is random and associated with a Rayleigh fading. Moreover,

the INR/SNR is set to 15 dB in Figures 6 and 8 and to 5dB for Figures 7 and 9. Note, in the presence of one interference, for both deterministic and random channels and for orthogonal synchronization sequences, a performance degradation of all the receivers with respect to the no interference case and the equivalence of GLRT2, E0-GLRT3 and E1-GLRT3 robust receivers, which outperform the non robust ones even for a low INR/SNR value. Note that, for both the deterministic and the random case, very similar Figures are also obtained for a Gaussian interference instead of a QPSK interference. This result shows that the type of interference does not modify the performance of the considered detectors both in the deterministic and the random case. Thus, a good point of the robust detectors is that they are also robust to the interference constellation. Besides, for a given SNR, the decrease of the INR increases the detection performance but does not modify the relative performance of the considered detectors.

Figure 6

Figure 7

Figure 8

Figure 9

Under the same assumptions as Figure 8 but for $(M, N) = (4, 4)$ and $(M, N) = (2, 8)$, Figure 10 shows, for $K'/K = 2$ and 10, the variations of P_M as a function of the SNR per receive antenna at the output of the GLRT2, GLRT2-CRD and E0-GLRT3-CRD receivers. Note an increasing performance degradation of GLRT2-CRD and E0-GLRT3-CRD with respect to GLRT2 (equivalent in this case to E0-GLRT3) as K'/K increases, while remaining lower than 1 dB for $K'/K = 2$, enlightening the interest of GLRT2-CRD and E0-GLRT3-CRD. Note also similar performance of GLRT2-CRD and E0-GLRT3-CRD receivers for $K'/K = 2$ and a better performance of E0-GLRT3-CRD with respect to GLRT2-CRD for $K'/K = 10$, showing a better robustness of the former.

Figure 10

b) *Non-orthogonal synchronization sequences*

For non-orthogonal sequences, we must consider the MMSE receiver in addition to the previous ones. Moreover, we also consider the COR receiver among the non-robust receivers. Under the previous assumptions, Figures 11 and 12 consider the same scenarios and show the same variations as Figures 4 and 5 respectively but in the presence of one interference. For Figure 11, the vector $\boldsymbol{h}_I$ is again associated with the DOA $\theta_I = 20°$, whereas for Figure 12, $\boldsymbol{h}_I$ is random and associated with a Rayleigh fading. Note increasing performance of all the receivers with both the SNR and N, despite the presence of a strong interference, and slightly decreasing performance of all the receivers with the correlation of the synchronization sequences. Note, for deterministic channels, the best behaviour of the MMSE receiver which is better than the GLRT2, E0-GLRT3 and E1-GLRT3 receivers which are practically equivalent. Note, for random channels, the best behaviour of the MMSE receiver with respect to the others, approximately equivalent, below a certain value of SNR, increasing with the number

of antennas. However, above this value of SNR, we note the best behaviour of GLRT2, E1-GLRT3 and E0-GLRT3, almost equivalent, which outperform the MMSE receiver. This analysis shows, in all cases, the practical interest of E1-GLRT3 and E0-GLRT3 with respect to GLRT2 receiver, since they behave similarly with a reduced complexity. It also shows the interest of MMSE receiver whatever the SNR for deterministic channels and at low SNR for random channels, jointly with its sub-optimality at moderate to high SNR for random channels.

Figure 11

Figure 12

9.4 Optimization of *M*

As the complexity of all the previous receivers increases with the number of transmit antennas M, it is important in practice to wonder whether this parameter can be optimized for synchronization purposes. In other words, one may wonder whether it exists an optimal number of transmit antennas for given propagation channel, number of receive antennas and interference scenario. We investigate this question in this section and we analyze in particular the conditions under which it becomes sub-optimal to implement a MIMO receiver with respect to a SIMO one, both without and with interference. For this purpose, we consider (MxN) MIMO links with either deterministic or random channel matrix H and we assume orthogonal synchronization sequences of K = 32 samples having the same power. In the presence of one interference, INR/SNR = 15 dB. $P_{FA} = 10^{-3}$ for all the scenarios and the figures are built from 10^6 independent realizations.

a) *Deterministic channels*

Under the previous assumptions, Figure 13 and 14 show, for deterministic channels, N = 4 and several values of M, the variations of P_M as a function of the SNR per receive antenna at the output of the GLRT2 receiver (similar results are obtained for E0-GLRT3 and E1-GLRT3 receivers) without and with an QPSK interference respectively. Note decreasing performance with increasing M in all cases and thus the optimality of SIMO receivers for synchronization through deterministic channels. In fact, for a given level of SNR at reception and in the absence of fading, increasing M does not create any spatial diversity but increases the number of transmitted sequences and thus the amount of interference at reception for each synchronization sequence. Hence the optimality of SIMO receivers.

Figure 13

Figure 14

b) *Random channels*

Figure 15 and 16 show the same variations as Figures 13 and 14 respectively under the same assumptions but for random channels. At low SNR, Figures 15 and 16 still show the optimality of the SIMO scheme for

synchronization, proving in this case that the dominant limitation parameter are the interferences. However, at higher SNR and for a given value of N, increasing M under the constraint of transmitting the same global power, should increase the spatial diversity order of the MIMO system for fading channels. However, increasing M also increases the number of transmitted sequences and thus the amount of interference at reception for each synchronization sequence. A compromize between diversity and interferences should then be found. Figures 15 and 16 show in this case, and for $N = 4$, the sub-optimality of the SIMO receiver due to fading and increasing performance with M as long as $M \leq M_o$, due to an increase of the system diversity order up to an optimal order, $N\,M_o$, which increases as the wanted P_M decreases. For $M > M_o$, i.e. above a system diversity order of $N\,M_o$, the fading has practically disappeared for the wanted P_M and the increase in diversity gain is very weak while the interference level increases, hence non increasing or even decreasing performance with M. Figure 15 shows that in the absence of interference, $M_o = 2$ for $2.10^{-2} \leq P_M \leq 10^{-1}$, whereas $M_o = 4$ for $10^{-3} \leq P_M \leq 2.10^{-2}$, which corresponds to an optimal system diversity order equal to 8 and 16 respectively. Similarly, in the presence of one interference, Figure 16 shows that $M_o = 2$ for $3.10^{-2} \leq P_M \leq 2\ 10^{-1}$, whereas $M_o = 4$ for $2.10^{-3} \leq P_M \leq 3.10^{-2}$, which again corresponds to an optimal system diversity order equal to 8 and 16 respectively.

Figure 15

Figure 16

10. CONCLUSION

In this paper, new insights into the time synchronization of (MxN) MIMO systems, without and with interference of any kind, have been given. In the absence of interference, the GLRT1 receiver has been computed for arbitrary synchronization sequences and have been compared to several receivers of the literature through a unified framework. While equivalent, for orthogonal synchronization sequences, to the COR and LS receivers, the GLRT1 receiver has been shown to be better than all the receivers of the literature for non-orthogonal sequences and random channels above a certain level of received SNR. In the presence of interference, several schemes aiming at reducing the complexity of the GLRT2 receiver presented in [30] and involving a determinant computation have been proposed. Two new receivers robust to interference, the E0-GLRT3 and E1-GLRT3 receivers, corresponding to two different estimates of the GLRT receiver in known, Gaussian, circular, temporally white and spatially colored noise, called GLRT3 receiver, have been introduced. These receivers have been shown to give performance very close to that of the GLRT2 receiver whatever the correlation of the sequences, with or without interference and for both deterministic and random channels. An additional powerful procedure of computation rate reduction of the data correlation matrix has been proposed for orthogonal sequences and for both the GLRT2 and the E0-GLRT3 receivers, giving rise to GLRT2-CRD and E0-GLRT3-CRD receivers respectively. The performance of these latter receivers have been shown to be close to that of the GLRT2 and the E0-GLRT3 receivers. A comparative complexity analysis of the considered receiver has been

presented for orthogonal synchronization sequences. From this point of view, the interest of E0-GLRT3 with respect to GLRT2 and of E0-GLRT3-CRD and GLRT2-CRD with respect to E0-GLRT3 and GLRT2 respectively has been shown to increase as Min(N, M) increases. Finally, the problem of optimization of the number of transmit antennas for time synchronization has been investigated for both deterministic and Rayleigh channels. For deterministic channels, without or with interference, SIMO receivers have been shown to be better than MIMO receivers. For random channels, while SIMO receivers are still optimal for low SNR, MIMO receivers become better than SIMO receivers for moderate and high SNR. In this case, for given values of N and P_M, it exists an optimal value, $M_{opt}(N, P_M)$, of the number of transmit antennas which gives the best performance. All these results should be useful to optimize the choice and the implementation of the receiver for time synchronization in practical systems.

APPENDIX A

It is shown in this appendix that expression (9) is a sufficient statistic for the GLRT detection of the known matrix S from observation matrix X, assuming zero-mean, stationary, i.i.d, spatially white, circular Gaussian samples $\boldsymbol{v}(k)$ ($1 \le k \le K$), and unknown parameters H and η_2. To this aim, let us first compute the ML estimates of (H, η_2) under H_1 and of η_2 under H_0 respectively. Using (8) and (6) for $R = \eta_2 I_N$, the Log-likelihood, Log(L_1), of (H, η_2) under H_1, observing X, can be written as

$$\mathrm{Log}[L_1] = -NK\mathrm{Log}(\pi) - NK\mathrm{Log}(\eta_2) - \sum_{k=1}^{K} [\boldsymbol{x}(k) - H\boldsymbol{s}(k)]^H[\boldsymbol{x}(k) - H\boldsymbol{s}(k)] / \eta_2 \qquad \text{(A1)}$$

Derivating this expression with respect to η_2 and setting the result to zero, we obtain the ML estimate, $\hat{\eta}_{21}$, of η_2 under H_1, given by

$$\hat{\eta}_{21} = \frac{1}{NK} \sum_{k=1}^{K} [\boldsymbol{x}(k) - H\boldsymbol{s}(k)]^H[\boldsymbol{x}(k) - H\boldsymbol{s}(k)] \qquad \text{(A2)}$$

In a similar way, it is easy to show that the ML estimate, $\hat{\eta}_{20}$, of η_2 under H_0 is given by

$$\hat{\eta}_{20} = \frac{1}{NK} \sum_{k=1}^{K} \boldsymbol{x}(k)^H\boldsymbol{x}(k) = \mathrm{Tr}(\hat{R}_x) / N = \hat{r}_x / N \qquad \text{(A3)}$$

Moreover, the ML estimate, $\hat{H}$, of H maximizes (A1) and is given by

$$\hat{H} = \hat{R}_{xs} R_s^{-1} , \qquad \text{(A4)}$$

Replacing in (8) (H, η_2) by ($\hat{H}$, $\hat{\eta}_{21}$) under H_1 and η_2 by $\hat{\eta}_{20}$ under H_0, we obtain the GLRT test, given by

$$\mathrm{GLRT} = \left(\frac{\hat{\eta}_{20}}{\hat{\eta}_{21}} \right)^{NK} \qquad \text{(A5)}$$

Developing (A2) and using (A3), it is straightforward to show that $\hat{\eta}_{21}$ takes the form

$$\hat{\eta}_{21} = \hat{\eta}_{20} - \frac{1}{N} \mathrm{Tr}(\hat{R}_{xs} R_s^{-1} \hat{R}_{xs}^{H}) \quad \text{(A6)}$$

Inserting (A6) into (A5), we deduce that a sufficient statistic for the previous problem is given by (9).

APPENDIX B

It is shown in this appendix that expression (22) is a sufficient statistic for the GLRT detection of the known matrix S from observation matrix X, assuming zero-mean, stationary, i.i.d, spatially colored, circular, Gaussian samples $\boldsymbol{v}(k)$ $(1 \le k \le K)$, a known matrix R and an unknown matrix H. The ML estimate, $\hat{H}$, of H under H_1 is still given by (A4). Replacing in (8) H by its ML estimate, using (6) and taking the Logarithm of (8) we find that a sufficient statistic for the previous problem is given by

$$K\,\mathrm{GLRT3} = \sum_{k=1}^{K} [\, 2\mathrm{Re}(\boldsymbol{s}(k)^{H} \hat{H}^{H} R^{-1} \boldsymbol{x}(k)) - \boldsymbol{s}(k)^{H} \hat{H}^{H} R^{-1} \hat{H} \boldsymbol{s}(k)] \quad \text{(B1)}$$

where Re[.] means real part. Using (A4) in (B1), we deduce that the sufficient statistic GLRT3 is defined by (22).

Acknowledgements

The authors would like to thank Prof. Philippe Loubaton for its valuable comments and suggestions that helped improve the quality of this manuscript. This work has been done through the CIFRE PHD contract of Sonja Hiltunen between CNRS, University of Marne La Vallee and Thales SIX GTS France.

REFERENCES

[1] G.J. FOSCHINI, M.J. GANS, "On limits of wireless communications in a fading environment when using multiple antennas", *Wireless Pers. Commun.*, Vol 6, N°3, pp. 311-335, 1998.

[2] E.I. TELATAR, "Capacity of multi-antenna Gaussian channels", *Europ. Trans. Comm.*, Vol 10, pp. 585-596, 1999.

[3] V. TAROKH, N. SESHADRI, A.R. CALDERBANK, "Space-time codes for high data rate wireless communication: performance criterion and code construction", *IEEE Trans. Inform. Theory*, Vol 44, N°2, pp. 744-765, March 1998.

[4] V. TAROKH, H. JAFARKHANI, A.R. CALDERBANK, "Space-time block codes from orthogonal designs", *IEEE Trans. Inform. Theory*, Vol 45, N°?, pp. 1456-1467, July 1999.

[5] S.N. DIGGAVI, N. AL-DHAHIR, A. STAMOULIS, A.R. CALDERBANK, "Great expectations: The value of spatial diversity to wireless networks", *Proc. IEEE*, Vol 92, No2, pp. 219-270, Feb. 2004.

[6] D. ASTELY, E. DAHLMAN, A. FURUSKAR, Y. JADING, M. LINDSTROM, S. PARKVALL, "LTE: The evolution of Mobile Broadband", *IEEE Communications Magazine*, pp. 44-51, April 2009.

[7] D. BAI, C. PARK, J. LEE, H. NGUYEN, J. SINGH, A. GUPTA, Z. PI, T. KIM, C. LIM, M-G. KIM, I. KANG, "LTE-Advanced Modem Design: Challenges and Perspectives", *IEEE Communications Magazine*, pp. 178-186, Feb. 2012.

[8] D. GESBERT, M. KOUNTOURIS, R.W. HEALTH, C.B. CHAE, T. SALZER, "From single-user to Multi-user Communications shifting the MIMO paradigm", *IEEE Signal Processing Magazine*, Vol. 24, N°5, pp. 36-46, Oct.. 2007.

[9] V.R. CADAMBE, S.A. JAFAR, "Interference Alignment and Degrees of freedom of the K-user Interference Channel", *IEEE Trans. On Info. Theory*, Vol. 54, N°8, pp. 3425-3441, Aug. 2008.

[10] A.N. MODY, G. L. STUBER, "Synchronization for MIMO OFDM systems", *Proc. Globecom'01,* Vol. 1, pp. 509-513, San Antonio, Nov. 2001.

[11] Y. ZHANG, S.L. MILLER, "Code Acquisition in transmit diversity DS-CDMA systems", *IEEE Trans. On Communication*, Vol 51, N° 8, pp. 1378-1388, Aug. 2003.

[12] A. VAN ZELST, T.C.W. SCHENK,"Implementation of a MIMO OFDM-Based Wireless LAN System", *IEEE Trans. On Signal Processing*, Vol 52, N° 2, pp. 483-494, Feb. 2004.

[13] G. L. STUBER, J.R. BARRY, S.W. MCLAUGHLIN, Y. LI, M.A. INGRAM, T.G. PRATT, "Broadband MIMO-OFDM Wireless Communications", *Proc. IEEE*, Vol 92, N° 2, pp. 271-294, Feb. 2004.

[14] E. ZHOU, X. ZHANG, H. ZHAO, W. WANG, "Synchronization Algorithms for MIMO OFDM systems", *Proc. IEEE Wireless Communications and Networking Conference* (WCNC'05), Vol 1, pp. 18-22, 2005.

[15] Z. MA, X. WU, W. ZHU, "An ICI-free Synchronization Algorithm in MIMO-OFDM System", *Proc. Int. Symposium Wireless Pervasive Computing* (ISWPC'07), pp. 242-246, Feb. 2007.

[16] A. SAEMI, J.P. CANCES, V. MEGHDADI, "Synchronization Algorithms for MIMO OFDMA Systems", *IEEE Trans. On Wireless Communications*, Vol 6, N° 12, pp. 4441-4451, Dec. 2007

[17] L. QI, H. BO, "Joint Timing Synchronization and Frequency-Offset Acquisition Algorithm for MIMO OFDM Systems", *Journal of Systems Engineering and Electronics*, Vol 20, N°3, pp. 470-478, 2009.

[18] C.L. WANG, H.C. WANG, "Optimized joint fine timing synchronization and channel estimation for MIMO systems", *IEEE Trans. On Communication*, Vol 59, N°4, pp. 1089-1098, April 2011.

[19] N. HAN, N. DU, Y. MA, "Research of Time-Frequency Synchronization in MIMO-OFDM System", *Proc. IEEE Symposium on Electrical and Electronics Engineering* (EEESYM'12), pp. 555-558, 2012..

[20] T.L. KUNG, K.K. PARHI, "Optimized joint timing synchronization and channel estimation for communications systems with multiple transmit antennas", *EURASIP Journal on Advances in Signal Processing*, 2013:139, pp. 1-12, 2013.

[21] M. MAREY, O.A. DOBRE, R. INKOL, "A novel blind block timing and frequency synchronization algorithm for Alamouti STBC", *IEEE Comm. Letters*, Vol 17, N°3, pp. 569-572, March 2013.

[22] Y. WU, S. CHAN, E. SERPEDIN, "Symbol timing estimation in space-time coding systems based on orthogonal training sequences", *IEEE Trans. On Wireless Communications*, Vol 4, N° 2, pp. 603-613, March 2005.

[23] K. RAJAWAT, A. CHATURVEDI, "A low complexity symbol timing estimator for MIMO systems using two samples per symbol", ", *IEEE Comm. Letters*, Vol 10, N°7, pp. 525-527, July 2006.

[24] D. WANG, J. ZHANG, "Timing Synchronization for MIMO-OFDM WLAN Systems", *Proc. IEEE Wireless Communications and Networking Conference* (WCNC'07), pp. 1178-1183, 2007.

[25] S.H. WON, L. HANZO, "Non-coherent code acquisition in the multiple transmit/multiple receive antenna aided single- and multi-carrier DS-CDMA downlink", *IEEE Trans. On Wireless Communications*, Vol 6, N° 11, pp. 3864-3869, Nov. 2007.

[26] S.H. WON, L. HANZO, "Analysis of serial-search-based code acquisition in the multiple-transmit/multiple-receive-antenna-aided DS-CDMA downlink", ", *IEEE Trans. On Vehicular Technology*, Vol 57, N° 2, pp. 1032-1039, March 2008.

[27] S.H. WON, L. HANZO, "Non-coherent and differentially coherent code acquisition in MIMO assisted DS-CDMA multi-path downlink scenatios", *IEEE Trans. On Wireless Communications*, Vol 7, N° 5, pp. 1585-1593, May 2008.

[28] T. TANG, R.W. HEATH, "A Space-Time Receiver With Joint Synchronization and Interference Cancellation in Asynchronous MIMO-OFDM Systems", *IEEE Trans. On Vehicular Technology*, Vol 57, N°5, pp. 2991-3005, Sept. 2008.

[29] S.H. WON, L. HANZO, "Initial and post-initial code acquisition in the noncoherent multiple-input/multiple-output-aided DS-CDMA downlink", ", *IEEE Trans. On Vehicular Technology*, Vol 58, N° 5, pp. 2322-2330, June 2009.

[30] D.W. BLISS, P.A. PARKER,"Temporal Synchronization of MIMO Wireless Communication in the presence of Interference", *IEEE Trans. On Signal Processing*, Vol 58, N°3, pp. 1794-1806, March 2010.

[31] Y. ZHOU, E. SERPEDIN, K. QARAGE, O. DOBRE, "On the Performance of Generalized Likelihood Ratio Test for Data-Aided Timing Synchronization of MIMO Systems", *Proc. IEEE International Conference on Communications* (ICC'12), Bucharest, pp. 43-46, 2012..

[32] T. KOIVISTO, V. KOIVUNEN, "Diversity Transmission of Synchronization Sequences in MIMO Systems", *IEEE Trans. On Wireless Communications*, Vol 11, N° 11, pp. 4048-4057, Nov. 2012.

[33] S. HILTUNEN, P. LOUBATON, P. CHEVALIER, "Large system analysis of a GLRT for detection with large sensor arrays in temporally white noise", *IEEE Trans. Signal Proc.*, Vol.63, N°20, pp. 5409-5423, Oct. 2015.

[34] L.E. BRENNAN, I.S. REED, "An adaptive array signal processing algorithm for communications", *IEEE Trans. Aerosp. Electronic Systems*, Vol 18, N°1, pp. 124-130, Jan 1982.

[35] D.M. DUGLOS, R.A. SCHOLTZ, "Acquisition of spread spectrum signals by an adaptive array", *IEEE Trans. Acou. Speech. Signal Proc.*, Vol 37, N°8, pp. 1253-1270, Aug. 1989.

[36] S. HILTUNEN, P. CHEVALIER, P. LOUBATON, "New Insights into Time Synchronization of MIMO Systems with Interference" *Eusipco'15*, Nice (France), Sept. 2015.

[37] H.L. VAN TREES, "Detection, Estimation and Modulation Theory – Part I", *John Wiley and Sons*, 1968

[38] D.C. CHU, "Polyphase codes with good periodic correlation properties", *IEEE Trans. Info. Theory*, Vol 18, N°4, pp. 531-532, 1972.

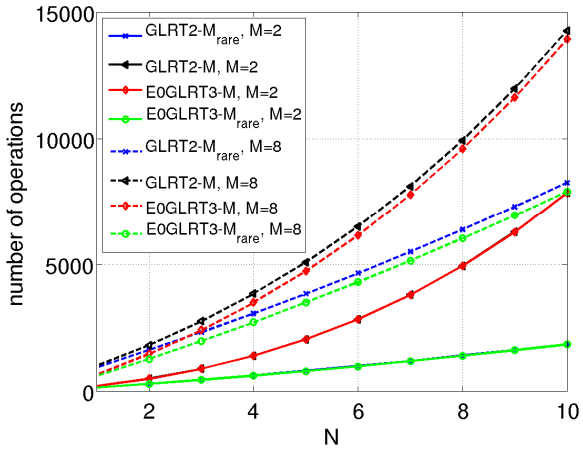

Figure 1 – *Number of complex operations from G_M as a function of N, K = 32, K'/K = 10*

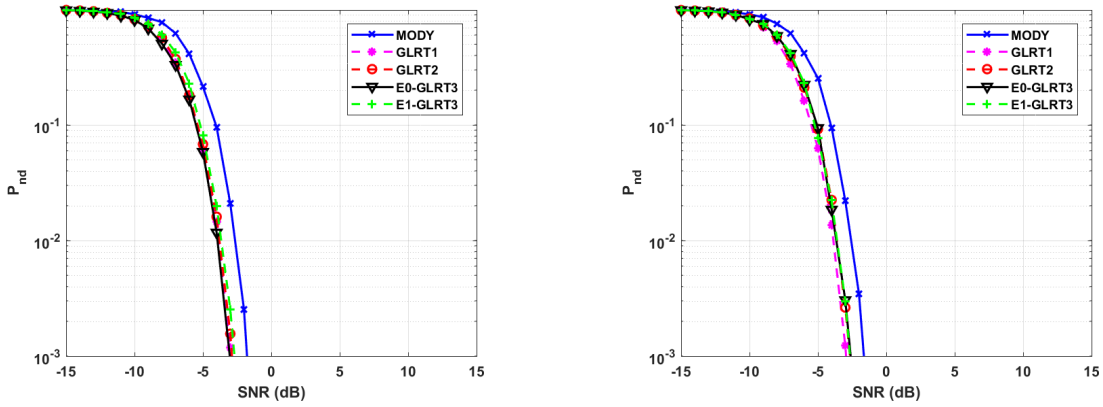

(a) (b)

Figure 2 – P_M *as a function of SNR, K = 32, M = N = 2,* $P_{FA} = 10^{-3}$*, No interference, Orthogonal sequences, Deterministic channel:* $|\alpha_{12}|^2 = 0$ *(a),* $|\alpha_{12}|^2 = 0.6$ *(b).*

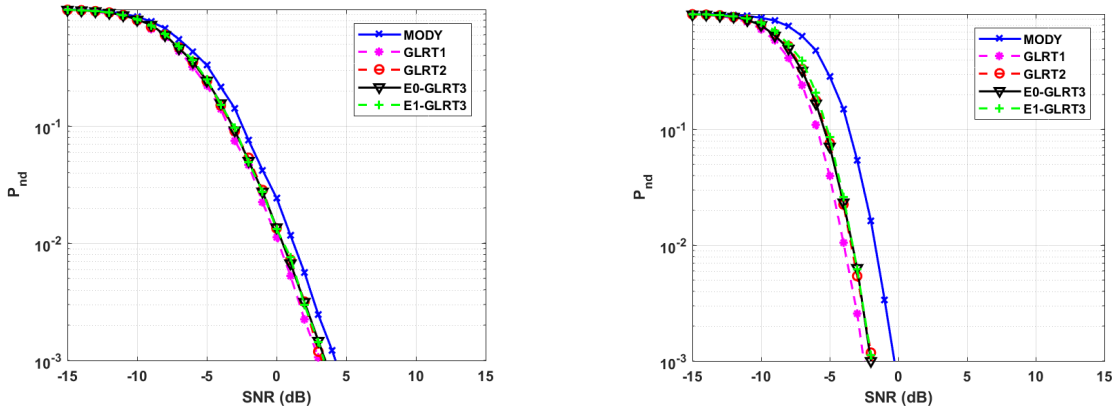

(a) (b)

Figure 3 – P_M *as a function of SNR, K = 32,* $P_{FA} = 10^{-3}$*, No interference, Orthogonal sequences, Random channel, M = N = 2 (a), M = N = 4 (b).*

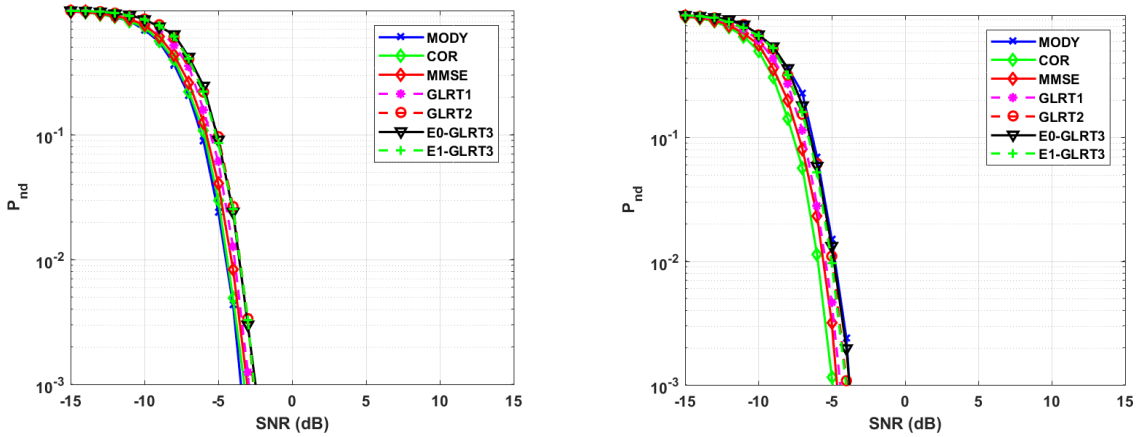

(a) (b)

Figure 4 – P_M *as a function of SNR, K = 32, M = N = 2,* $P_{FA} = 10^{-3}$*, No interference, Non-Orthogonal sequences, Deterministic channel:* $|\alpha_{12}|^2 = 0$ *(a),* $|\alpha_{12}|^2 = 0.6$ *(b).*

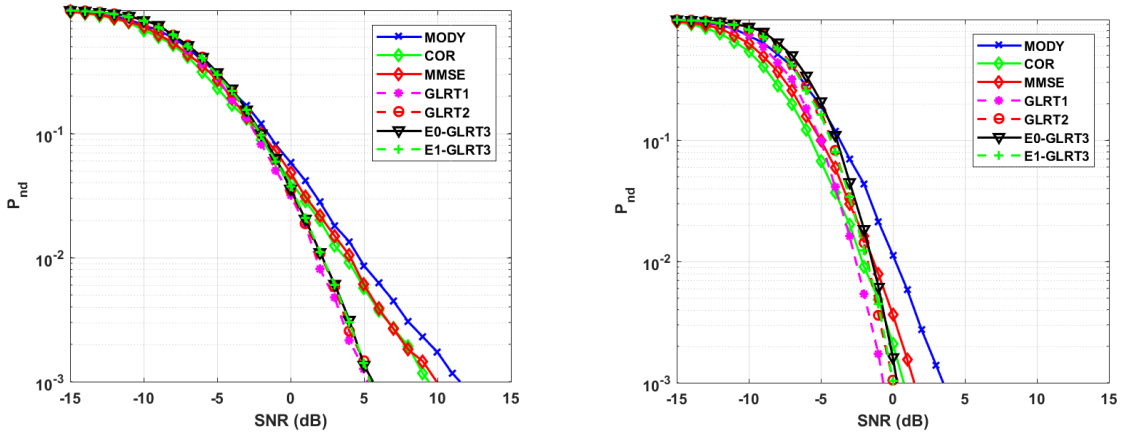

(a) (b)

Figure 5 – *P_M as a function of SNR, K = 32, $P_{FA} = 10^{-3}$, No interference, Non-Orthogonal sequences, Random channel, M = N = 2 (a), M = N = 4 (b).*

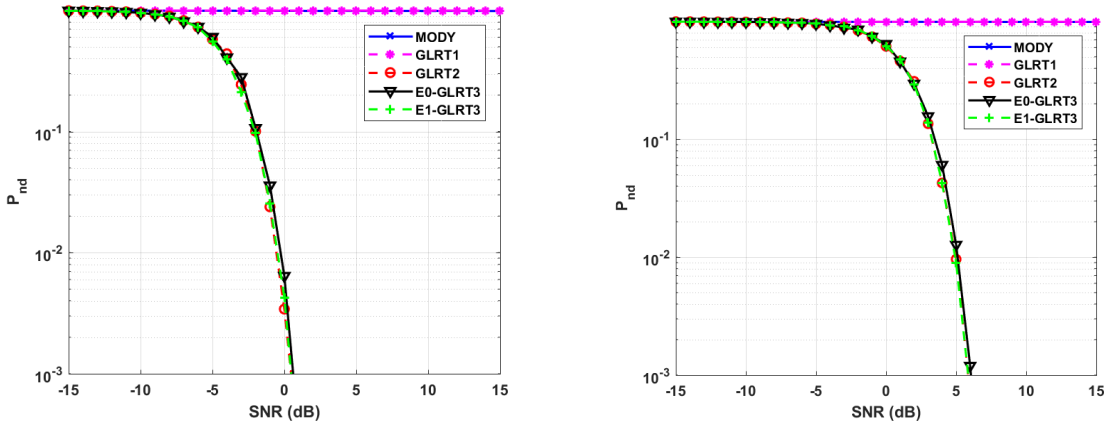

(a) (b)

Figure 6 – *P_M as a function of SNR, K = 32, M = N = 2, $P_{FA} = 10^{-3}$, One interference, INR/SNR = 15 dB, Orthogonal sequences, Deterministic channel:* $(|\alpha_{12}|^2, |\alpha_{1I}|^2, |\alpha_{2I}|^2) = (0, 0.74, 0.001)$ *(a),* $(|\alpha_{12}|^2, |\alpha_{1I}|^2, |\alpha_{2I}|^2) = (0.6, 0.74, 0.97)$ *(b)*

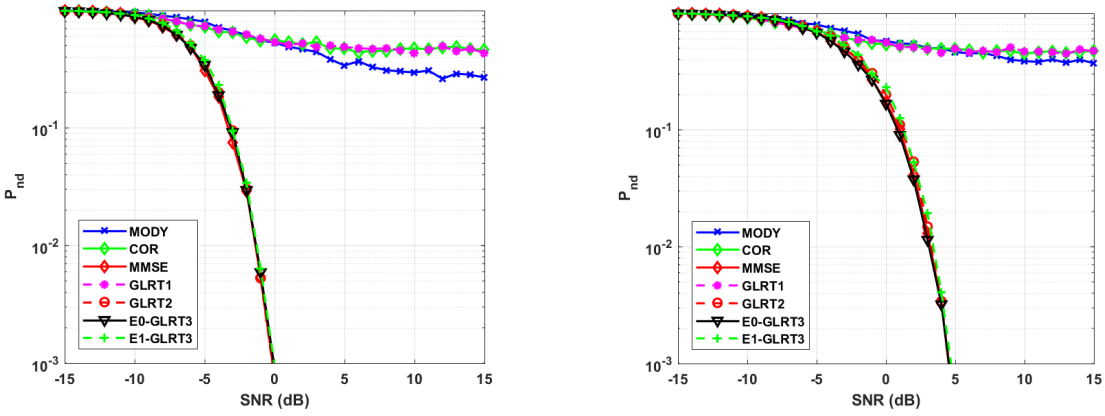

(a) (b)

Figure 7 – *P_M as a function of SNR, K = 32, M = N = 2, $P_{FA} = 10^{-3}$, One interference, INR/SNR = 5 dB, Orthogonal sequences, Deterministic channel:* $(|\alpha_{12}|^2, |\alpha_{1I}|^2, |\alpha_{2I}|^2) = (0, 0.74, 0.001)$ *(a),* $(|\alpha_{12}|^2, |\alpha_{1I}|^2, |\alpha_{2I}|^2) = (0.6, 0.74, 0.97)$ *(b)*

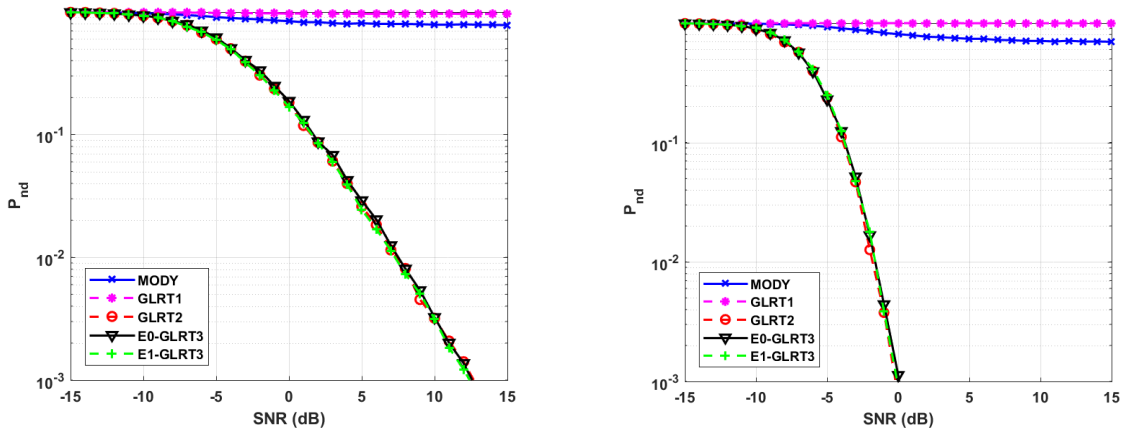

(a) (b)

Figure 8 – P_M *as a function of SNR, K = 32,* $P_{FA} = 10^{-3}$*, One interference, INR/SNR = 15 dB, Orthogonal sequences, Random channel, M = N = 2 (a), M = N = 4 (b).*

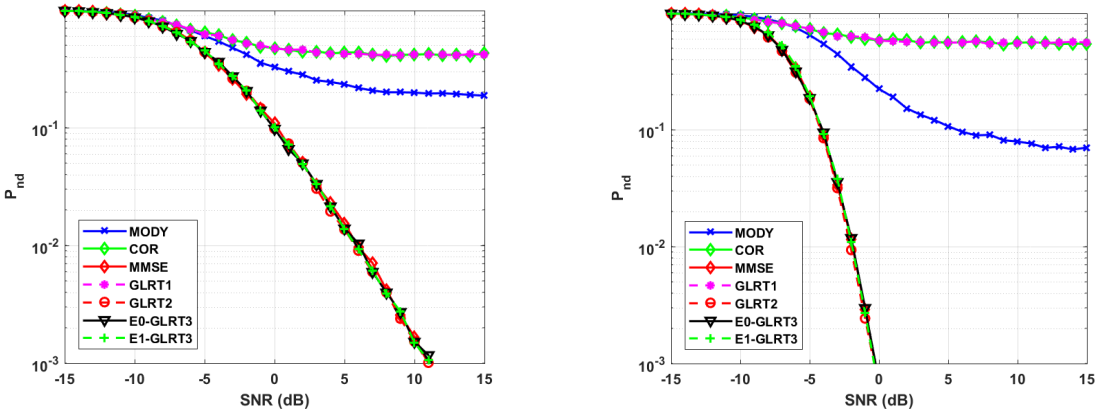

(a) (b)

Figure 9 – P_M *as a function of SNR, K = 32,* $P_{FA} = 10^{-3}$*, One interference, INR/SNR = 5 dB, Orthogonal sequences, Random channel, M = N = 2 (a), M = N = 4 (b).*

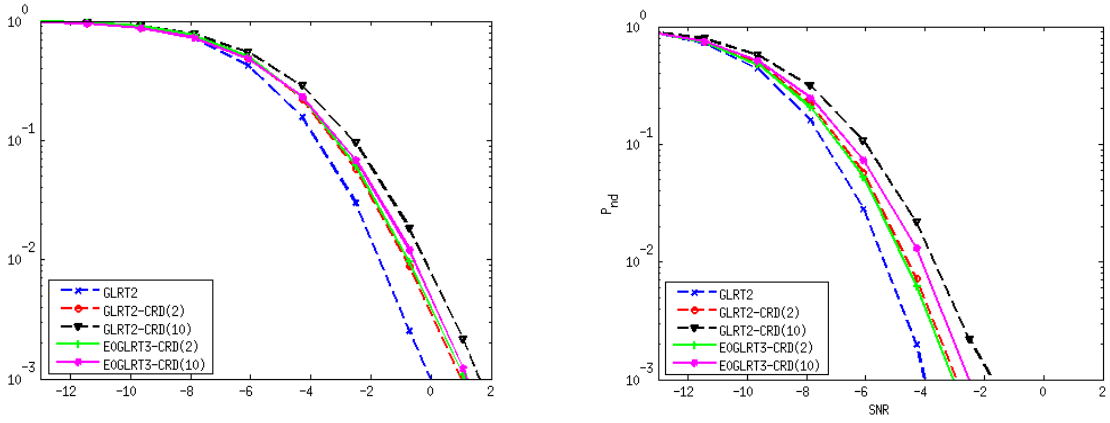

(a) (b)

Figure 10 – P_M *as a function of SNR, K = 32,* $P_{FA} = 10^{-3}$*, One interference, INR/SNR = 15 dB, Orthogonal sequences, Random channel,* $(M, N) = (4, 4)$ *(a),* $(M, N) = (2, 8)$ *(b).*

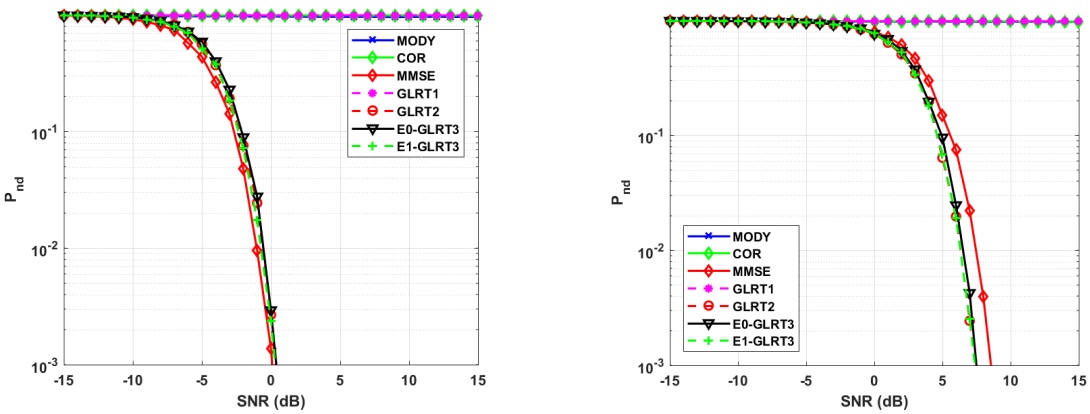

(a) (b)

Figure 11 – *P_M as a function of SNR, K = 32, M = N = 2, $P_{FA} = 10^{-3}$, One interference, INR/SNR = 15 dB, Non-orthogonal sequences, Deterministic channel:* $(|\alpha_{12}|^2, |\alpha_{1I}|^2, |\alpha_{2I}|^2) = (0, 0.74, 0.001)$ *(a),* $(|\alpha_{12}|^2, |\alpha_{1I}|^2, |\alpha_{2I}|^2) = (0.6, 0.74, 0.97)$ *(b)*

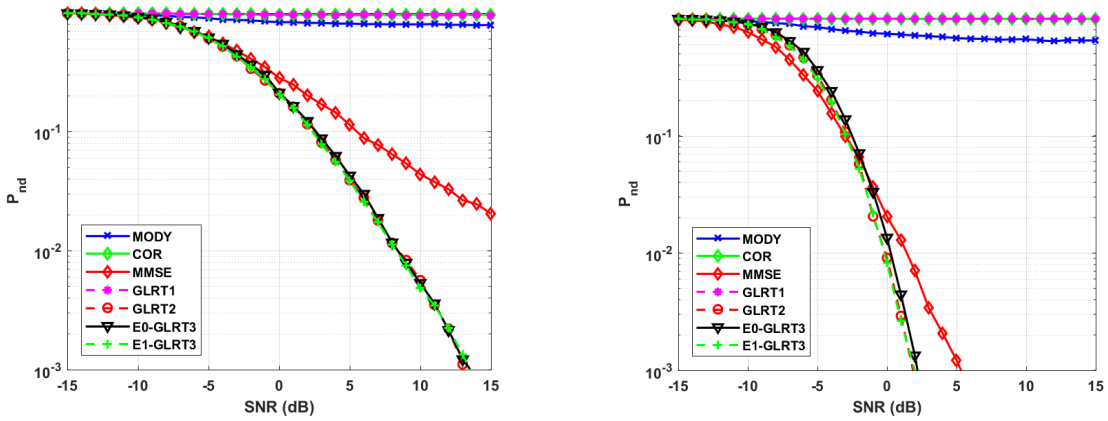

(a) (b)

Figure 12 – *P_M as a function of SNR, K = 32, $P_{FA} = 10^{-3}$, One interference, INR/SNR = 15 dB, Non-orthogonal sequences, Random channel, M = N = 2 (a), M = N = 4 (b).*

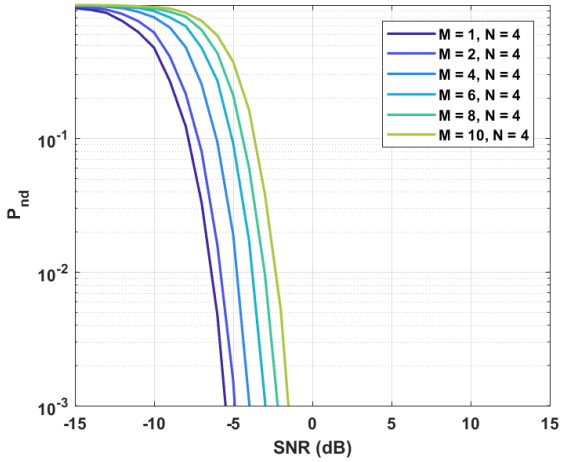

Figure 13 – *P_M as a function of SNR, K = 32, N = 4, Orthogonal sequences, Deterministic channel, No interference*

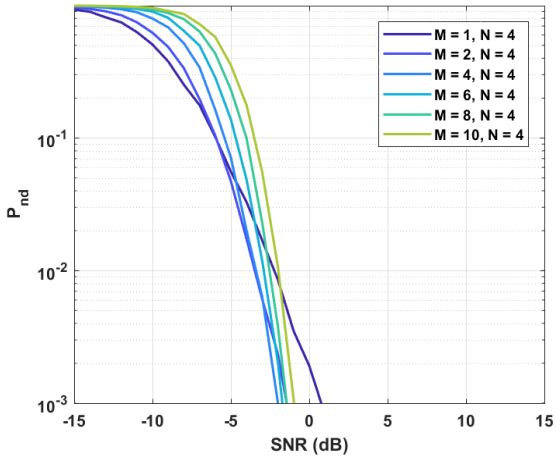

Figure 14 – P_M *as a function of SNR, K = 32, N = 4, Orthogonal sequences, Deterministic channel, One interference*

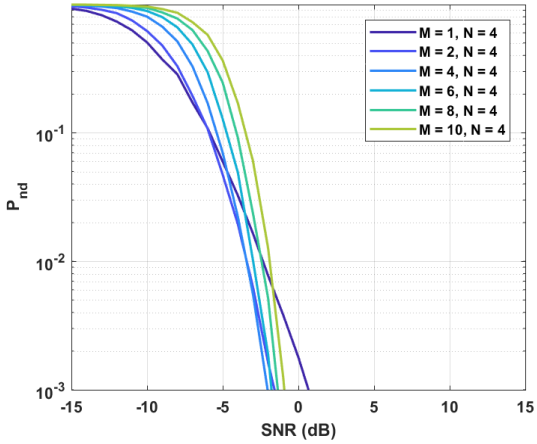

Figure 15 – P_M *as a function of SNR, K = 32, N = 4, Orthogonal sequences, Random channel, No interference*

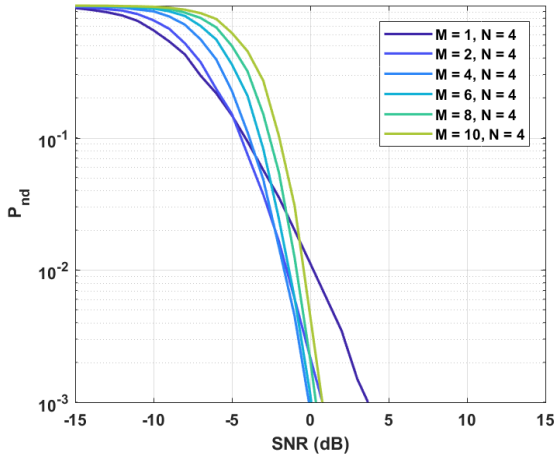

Figure 16 – P_M *as a function of SNR, K = 32, N = 4, Orthogonal sequences, Random channel, One interference*

	Trace/Det	Inverse	Matrix products
GLRT2	$2M^3/3 + 2M - 1$	$8N^3/3$	$MN(2K-1) + N(N+1)(2K-1)/2 + MN(2N-1) + M^2(2N-1)$
E0-GLRT3	$M - 1$	$8N^3/3$	$MN(2K-1) + N(N+1)(2K-1)/2 + MN(2N-1) + M^2(2N-1)$
GLRT2-CRD	$2M^3/3 + 2M - 1$	$8N^3/3\beta$	$MN(2K-1) + N(N+1)(2K-1/\beta)/2 + MN(2N-1) + M^2(2N-1)$
E0-GLRT3-CRD	$M - 1$	$8N^3/3\beta$	$MN(2K-1) + N(N+1)(2K-1/\beta)/2 + MN(2N-1) + M^2(2N-1)$

Table 1 – *Number of complex operations required by different receivers using* G_M